MASTER

BNL-23330

October 1977

CONF-771080--1

Charge Density Wave Instabilities and Incommensurate Structural Phase Transformations

J. D. Axe

NOTICE
This report was prepared as an account of work sponsored by the United States Government. Neither the United States nor the United States Department of Energy, nor any of their employees, nor any of their contractors, subcontractors, or their employees, makes any warranty, express or implied, or assumes any legal liability or responsibility for the accuracy, completeness or usefulness of any information, apparatus, product or process disclosed, or represents that its use would not infringe privately owned rights.

By acceptance of this article, the publisher and/or recipient acknowledges the U.S. Government's right to retain a nonexclusive, royalty-free license in and to any copyright covering this paper.

DISTRIBUTION OF THIS DOCUMENT IS UNLIMITED

BNL-23330
IAEA-SM-219/130

CHARGE DENSITY WAVE INSTABILITIES AND INCOMMENSURATE STRUCTURAL PHASE TRANSFORMATIONS*

17 - 21 October 1977
Vienna, Austria

Charge Density Wave Instabilities and Incommensurate Structural Phase Transformations*

J. D. Axe
Brookhaven National Laboratory, Upton, New York 11973

Incommensurate structural phase transformations involve the appearance of modulated atomic displacements with spatial periodicity unrelated to the fundamental periodicity of the basic lattice. In the case of some quasi one- or two-dimensional metals such transformations are the result of Fermi-surface instabilities that also produce electronic charge density waves (CDW's) and soft phonon modes due to metallic electron screening singularities. Incommensurate soft mode instabilities have been found in insulators as well. Recent neutron scattering studies of both the statics and dynamics of incommensurate structural instabilities will be reviewed.

1. INTRODUCTION

The most characteristic feature of incommensurate solid structures is their diffraction patterns, which consist of primary or parent Bragg reflections in a regular array in reciprocal space, but with each of these reciprocal points acting as an origin for a secondary set of satellite reflections with their own spacing. The parent reflections arise from an average structure. The true atomic positions differ from those of the average structure by an additional modulating displacement field characterized by a wave vector $\vec{q}$ which is incommensurate with the parent reciprocal lattice, i.e.

$$\vec{q} = x_1\vec{a}_1^* + x_2\vec{a}_2^* + x_3\vec{a}_3^*$$

* Research supported by the U. S. Department of Energy under Contract No. EY-76-C-02-0016.

where one or more of the x_i is an irrational number. It happens often that the amplitude of the modulation is small and can for most purposes be represented by a simple sinusoid. It is also not uncommon for the modulations to disappear above a certain temperature, i.e. the material may transform from an incommensurate structure to a commensurate one given by the average structure. This review is concerned with neutron scattering studies of such incommensurate phase transformations, and what they reveal of the nature of incommensurate instabilities.

Perhaps one of the simplest ways of viewing an incommensurate phase transformation is as a soft phonon mode instability. Although introduced to explain ferroelectric ($\vec{q}=0$) transformations[1], the idea was subsequently generalized to include instabilities at special symmetry points on the Brillouin zone boundary.[2] Indeed, such wave vectors are predisposed to instabilities in the sense that they represent extrema in the phonon dispersion surfaces, a necessary condition for a soft mode instability. Although certain extrema follow necessarily from symmetry, there are no restrictions on the number or position of additional minima which are possible.

On a more microscopic level, such an incommensurate transformation may result from a charge density wave instability[3] in the conduction electrons near the Fermi surface of a metal. The occurrence of such an electronic instability requires a large electronic susceptibility $\chi_o(\vec{q}_c)$ which is favored when large portions of the Fermi surface are separated by the special wave vector $\vec{q}_c$. This favorable nesting of the Fermi surface is much more probable for quasi one- or two-dimensional metals where the Fermi surface becomes independent of some components of electron momenta. The CDW instability is coupled to the phonons because of the screening effect of the conduction electrons on the "bare" phonon frequencies, $\Omega_{\vec{q}}$. In the random phase approximation, the observed physical phonon frequencies $\omega(\vec{q})$ are roughly of the form

$$\omega^2(\vec{q}) = \Omega^2(\vec{q}) \left[\frac{1 - \lambda_{\vec{q}}^2 \chi_o(\vec{q})}{1 - v_{\vec{q}}\, \chi_o(\vec{q})} \right]$$

where $\lambda_{\vec{q}}$ is an electron-phonon coupling constant and $v_{\vec{q}}$ is a Fourier component of the electron-electron interaction. Theory thus predicts the CDW instability to be accompanied by a soft phonon $(\vec{q}_c) \to 0$, where $\vec{q}_c$ is determined by the Fermi surface nesting. The phonon softening can be viewed as a giant Kohn anomaly.[4] Neutrons scatter not directly from the CDW but rather from the nuclear distortions resulting from the condensed phonon mode. (From a theoretical viewpoint, a mixed spin and charge density wave appears possible, but no spin components have yet been detected in CDW's.)[5]

At least from a mathematical point of view, incommensurate structures are not crystalline, for they lack the required translational symmetry. Of course, these structures belong to no three-dimensional space groups. Recent work[6,7] has shown that it is possible to assign these structures to space groups of higher dimension. Physically, these extra dimensions relate to the evolution of the structure upon change of phase of the modulation relative to the parent structure.

2. CDW's IN TWO DIMENSIONS (TRANSITION METAL CHALCOGENIDES)

Within the past several years, evidence has accumulated pointing to the existence of CDW instabilities in a number of layered transition metal chalcogenides. The literature up to 1974 has been extensively reviewed by Wilson et al.[8], and subsequent developments are reviewed by Di Salvo[9], and Moncton, Axe, and Di Salvo.[10] The materials we discuss have a chemical formula MX_2, where X = S, Se, or Te and primarily M = V, Nb, or Ta (group Vb). These materials crystallize into layered structures of which the basic structural unit is a layer of metal atoms sandwiched between two chalcogen layers. The layers are hexagonally packed and depending upon whether the two X-layers are eclipsed or staggered when viewed normal to the plane, the metal atoms show octahedral (O) or trigonal prismatic (TP) coordination. These three-layer units are held together by weak van der Waals X-X bonds and different structural modifications (polytypes) are possible depending upon the stacking sequence of O and TP layers.

2.1. 2-H Polytypes

In many respects the behavior of the so-called 2H-polytypes, which consists of entirely TP layers is the best studied. Electron diffraction studies of both 2H-$NbSe_2$ and $TaSe_2$ showed satellite reflections appearing at low temperature.[8] These peaks were originally thought to be commensurate with a spacing of 1/3 of the basal plane reciprocal lattice spacing $\vec{a}_H^*$, but a subsequent neutron diffraction study[10] showed that the ordering, which occurs at a well-defined temperature, leads initially to incommensurate structures with wave vectors $\vec{q}_\delta = (1-\delta)\vec{a}_H^*/3$ with $\delta \sim 0.02$ at the transformation temperatures (T_o = 33.4 K and 122.3 K for $NbSe_2$ and $TaSe_2$, respectively). The temperature dependence of the satellite intensities which is proportional to the square of the CDW amplitude is shown in Fig. 1. The transformations appear to be continuous (i.e. second order) although it is impossible to rule out the possibility of a small first-order discontinuity.

The temperature dependence of the CDW wave vector is shown in Fig. 2 and establishes that although the CDW remains incommensurate in $NbSe_2$, in $TaSe_2$ there is an apparently discontinuous transformation at $\sim$ 90 K in which $\delta \to 0$ and the superlattice remains commensurate below this temperature.

By studying the intensity of the satellite reflections, Moncton et al.[10] deduced a pattern of ionic displacements in $TaSe_2$ at 5 K shown in Fig. 3. The displacement pattern can be understood as the condensation of a single (predominantly longitudinal) phonon. To be more precise, three phonon modes with wave vectors related by a three-fold rotation about the c-axis are required. A combination of diffraction and other evidence establish that all three wave vectors are simultaneously present on a microscopic level in the crystal. The displacement pattern has a pronounced optic mode character involving opposing Se- and Ta-atom motion. This undoubtedly reflects the fact that the cations and anions move in opposite directions under the Coulomb field established by the CDW.

The relatively small size of the available crystals has limited the inelastic neutron scattering to the lowest phonon branches. The most striking effect is a pronounced softening of the LA phonons propagating along $\vec{a}_H^*$. This branch has the same symmetry character (Σ_1) as the static displacements discussed above. As seen in Fig. 4, the wave vector minimum is very close

to $\vec{a}_H^*$ as would be expected. This minimum is very insensitive to the c-axis component of momentum transfer, implying strong two-dimensional character. The square of the measured phonon frequencies at the mimimum is plotted vs. temperature in Fig. 5. It is apparent that there is appreciable softening above T_o, and that this is reversed below T_o. It appears that the mode softening is far from complete at T_o, although the relatively poor experimental resolution may act to reduce the apparent sharpness of the anomaly.

In addition to the inelastic scattering discussed above, there is also diffuse quasi-elastic critical scattering peaking near $\vec{q}_\delta$ and at $T \gtrsim T_o$. It is only moderately anisotropic, the ratio of the inverse correlation lengths parallel and perpendicular to the basal plane $\kappa_{||}/\kappa_{\perp} \sim 1/3$.

2.2. Other Polytypes

The behavior of the CDW's in other polytypes is quite different from that of the 2H modifications. Electron-diffraction studies show that the 1T polytype (all O-type layers) of $TaSe_2$ has an incommensurate CDW onset temperature in excess of 600 K.[8] The wave vector is $q \gtrsim 0.285\ \vec{a}_H^*$ shorter than for the 2H polytypes. It also exhibits a lock-in transformation, but of a more complicated type, whereby $\vec{q}$ rotates by $\sim 13.9°$ away from the trigonal axis to produce a 3 x 1 superlattice. The component of the CDW wave vector in the basal plane has a magnitude $\sqrt{13}\ \vec{a}_H^*$. The CDW pattern for one layer is shown in Fig. 6.

In the 4Hb polytype of $TaSe_2$ O and TP layers alternate. Electron and neutron diffraction studies[11] establish that the differently coordinated layers undergo independent transformations to CDW states similar to 1T- and 2H-$TaSe_2$. Although the O-CDW's exhibit three-dimensional ordering, the TP-CDW's are uncorrelated from plane to plane.

Adjacent CDW layers stack in such a way as to minimize their interaction energy. For the incommensurate 1T-structure, this is accomplished by placing the maximum of the CDW for layers $\ell \pm 1$ over the minima which occur in the ℓ'th layer, i.e. at positions B and C of Fig. 6. However, in the commensurate case, the CDW maxima cannot be shifted arbitrarily, but must coincide with a metal atom position. The simple ABC stacking sequence must be modified by placing the CDW maxima in say layer $\ell + 1$ at one of the three metal positions closest to B. Moncton et al.[11] have done a neutron diffraction study of the effect of impurities on the CDW stacking order in 1T-$TaSe_2$. For small Ze impurity concentrations ($\lesssim 0.015\%$), they find the ordered stacking sequence described above which gives sharp Bragg reflections at $\vec{q} = 2/13\ \vec{c}_H^*$, $5/13\ \vec{c}_H^*$ and $6/13\ \vec{c}_H^*$ (see Fig. 7). Higher impurity concentrations cause a broadening and shifting of the reflections, leading finally to a single peak at $1/3\ \vec{c}_H^*$. These data can be understood quantitatively by a simple model in which random impurity effects dominate the next-nearest-layer interaction, causing a disordered stacking sequence involving translations of successive CDW maxima among the three positions that border the B and C positions in Fig. 6.

3. CDW's IN ONE DIMENSION (PEIERLS TRANSFORMATION)

In quasi one-dimensional metals, the Fermi surface approaches a set of parallel planes oriented perpendicular to the one-dimensional axis and separated by $2k_F$. This is the most geometrically favorable situation for CDW with nesting occurring over the whole Fermi surface. It is often called

a Peierls transformation, since Peierls first studied it in the mean field approximation long before physical manifestations were known.[13]

The interest, particularly from a theoretical point of view has been enormous since a 1-d electron gas has many exactly calculable and unusual properties.[14,15] The experimental situation vis-a-vis scattering experiments has been recently reviewed by Comès and Shirane.[16] The systems studied thus far fall naturally into two groups with rather different properties.

3.1. Linear Platinum Complexes (KCP)

Beyond any doubt the most spectacular demonstration to date of the influence of a nearly one-dimensional Fermi surface on phonons is provided by KCP. $K_2Pt(CN)_4Br_x \cdot rH_2O$(KCP) has a tetragonal structure in which square planar $Pt(CN)_4$ complexes are stacked along the c-axis with a Pt-Pt distance comparable to that in Pt metal. The nonstoichiometric Br^- ions ($x \approx 0.3$) are distributed randomly in the lattice and deplete the highest Pt bonding orbitals to form a one-dimensional conduction band, with $|\vec{k}_F|$ proportional to x.

3.1.1. Inelastic Scattering

Following a familiar pattern, evidence for unusual excitations came first from x-ray studies[17] which established the presence of sheets of diffuse scattering in reciprocal space at $2\vec{k}_F = 0.3(\text{mod } \vec{c}^*)$. Subsequent neutron scattering studies[18] showed that at high temperatures this arises predominantly from a giant Kohn anomaly in the acoustic phonons. The remarkable nature of the phonon dispersion is well represented by Fig. 8.[19] The anomaly is so sharply confined along $\vec{c}^*$ that a conventional representation in terms of a sharp phonon dispersion surface is not possible with existing experimental resolution. The most detailed summary of results near the anomaly take the form of intensity contour maps such as shown in Fig. 9. From a series of such measurements Carneiro et al.[20] conclude that there is a quasi-elastic peak at all temperatures but that below $\sim$ 160 K there is an additional inelastic maximum at $\sim$ 2.5 meV, which becomes increasingly well separated from the quasi-elastic scattering as the temperature is lowered. They ascribe the disappearance of this gap at higher temperatures to phonon lifetime effects, and thus conclude that the phonon frequency does not vanish at any temperature.

3.1.2. Quasi-elastic Scattering

As mentioned above, the quasi-elastic component of the diffuse scattering is weak but noticeable at higher temperatures ($T \gtrsim 150$ K) and is essentially uniform over the $2\vec{k}_F$ Bragg "planes" when corrected for structure factor effects. As the temperature is lowered, however, peaks begin to develop at $(h + 1/2,\ k + 1/2,\ \ell \pm 2\vec{k}_F)$ indicating that the fluctuations on the chains are no longer random but tend to correlate in such a way that fluctuations on near-neighbor chains are out of phase. The temperature dependence of the intensity as well as the transverse ($\perp$ to $\vec{c}^*$) width of this scattering is shown in Fig. 10.[21] The finite T-independent width below $\sim$ 100 K indicates that true long range order is never achieved, the transverse correlation range reaches a maximum of $\sim$ 100 Å. (The correlation length along a chain was too long to be measurable (> 300 Å) at all temperatures.) Nevertheless, the marked variation in the peak width seen in

Fig. 10 indicates an incipient phase transformation with $T_c \approx 100$ K.

It is well known that true one-dimensional systems cannot achieve long-range order at any finite temperature. Nevertheless, weak interchain coupling removes this restriction and a "weak" three-dimensional system is expected to order at a temperature given by

$$kT_c \approx 2J_{//}/\ln(J_{//}/J_{\perp})$$

where $J_{//}$ and $J_{\perp}$ measure respectively the intrachain and interchain interaction.[22] This would predict a reasonable transition temperature for KCP. The reason for the failure to attain long-range order may be due to the effect of the random potential of the Br ions.

3.2. Organic Metals (TTF-TCNQ)

Although the striking d.c. conductivity anomalies reported[23] in 1973 set off an extensive search for phase transformations in this material and related compounds, direct structural information for a phase transformation was delayed because of experimental difficulties in performing x-ray measurements below liquid nitrogen temperatures, and because the small size of available single crystals was far from optimal for even elastic neutron scattering studies. In 1975 two independent x-ray scattering experiments revealed modulated long-range order in TTF-TCNQ at low temperatures, as well as diffuse scattering characteristic of one-dimensional fluctuations.[24,25] The nature of the long-range order was subsequently refined by a series of neutron scattering measurements.[26-28] The situation regarding the diffuse precursor scattering is not yet entirely understood, in part due to the extreme difficulty of inelastic neutron scattering on samples with a volume $\lesssim 0.05$ cm^3.

In order to comprehend the CDW behavior of TTF-TCNQ it is essential to have some familiarity with the crystal structure. TTF-TCNQ is an organic salt composed of a tetrathiafulvalene (TTF^+) cation and a tetracyanoquinodimethane ($TCNQ^-$) anion, both of which are planar aromatic molecules which stack in a plate-like structure shown in Fig. 11.[29] Chains of TTF or TCNQ molecules lie along the monoclinic b-direction which, because of overlapping π-orbitals is the direction of high conductivity. TTF and TCNQ chains alternate along the a-axis.

3.2.1. Elastic Neutron Scattering

As was established by Ellenson et al.[27], TTF-TCNQ goes through a sequence of three low temperature phase transformations. These transformations delineate four distinct phases whose properties are reflected in the position of the satellite Bragg reflections. These are given below with reference to the unmodulated reciprocal lattice vector ($hk\ell$).

I	$T > 54$ K	(unmodulated phase , no satellite reflections)
II	$54\ K > T > 48.5$ K	$(h \pm 0.5, k \pm 0.295, \ell \pm 0)$
III	$48.5\ K > T > 38$ K	$(h \pm (T), k \pm 0.295, \ell \pm 0)$
IV	$38\ K > T$	$(h \pm 0.25, k \pm 0.295, \ell \pm 0)$

The behavior of the satellite wave vector is shown in Fig. 12. Note that there is hysteresis in region III amounting to ~ 1 K in the best samples, but somewhat sample dependent. Phenomenological theories for

these phase transformations have been proposed.[30-32] It appears that at 54 K CDW order develops (predominantly) on the TCNQ chains in such a way that the CDW on adjacent chains is "out-of-phase." This accounts for the displacement of the satellites by 0.5 along a*. The wave vector along the chains (i.e. along $\vec{b}^*$) is determined by the nearly one-dimensional Fermi surface, $2\vec{k}_F = 0.295\ \vec{b}^*$, and this component of the satellite wave vector is temperature independent. Below 48.5 K, out of phase CDW's begin to develop on the TTF chains as well, and as first shown by Bak and Emery[30], the interaction between the CDW's on the two types of chains requre that the phases shift along $\vec{a}$. This accounts for the temperature dependent wave vector in region III. Finally, there is additional commensurability energy which locks the a* component of the wave vector at 0.25 below 38 K.

3.2.2. Inelastic Neutron Scattering

Diffuse planes of strongly temperature dependent x-ray scattering are observed below ∿ 150 K, with the wave vector $2\vec{k}_F = 0.295\ b^*$. Atomic displacements with components along both b* (longitudinal) and c* are observed. The inelastic neutron scattering data on deuterated samples[33,34] show a distinct (but rather weak compared with KCP) dip in the TA branch with(mostly) c*-axis polarization. See Fig. 13. At the minimum, the phonon energy decreases somewhat with decreasing temperature, but appears to remain > 4 meV. If there is any anomalous dip in the LA branch at $2\vec{k}_F$, it is considerably weaker than for TA(c*), and the energies increase with increasing temperature. There is likewise no evidence for anomalies in the remaing TA(a*) mode. The room temperature dispersion of all of the acoustic phonons propagating along $\vec{b}^*$ is shown in Fig. 13. It is not clear whether there is additional quasi-elastic scattering at $2\vec{k}_F$.

Additional strong diffuse x-ray scattering is seen at $4\vec{k}_F = 0.59\ \vec{b}^*$.[35,36] This scattering has a different temperature dependence from that at $2\vec{k}_F$, in that it persists to much higher temperatures. This has been searched for by neutrons and is as yet undetected.

A very sharp and deep Kohn-like anomaly in the LA-branch at $2\vec{k}_F$ was initially reported in protonated samples at room temperature by Mook and Watson.[37] This is not evident in the deuterated material.[38] It is not likely that this is connected with a CDW, for little or no diffuse scattering is seen at room temperature in the x-ray studies. It has been suggested that this scattering could arise from a spin density wave if the Coulomb interaction between electrons on adjacent molecules in a chain is sufficiently large.[39] This model predicts CDW excitations at $4k_F$, and thus furnishes a possible explanation of the diffuse x-ray scattering at this wave vector. However, it is at present controversial as to whether the necessary model parameters are reasonable. Since further experimental measurements raise questions as to the statistical reliability of the original neutron study, it seems that the matter may be decided only with the advent of larger samples.

4. INSULATORS

In low dimensional metals the forces responsible for the instability are due to ion-electron-ion interaction and are long ranged and oscillatory. The result, as we have seen, can be a sharp anomaly about $\vec{q}_c = 2\vec{k}_F$. In insulators studied thus far, the effective interaction ranges are shorter, leading to broader phonon anomalies which are very conveniently studied by

inelastic neutron scattering. In insulators, there is no essential requirement for incommensurate instabilities which favors low spatial dimensionalities and indeed the known examples lack any obvious lower pseudo-dimensionality.

4.1. K_2SeO_4

The most detailed neutron scattering study to date on an insulating incommensurate structure has been performed on K_2SeO_4 by Iizumi et al.[40] The high temperature unmodulated structure is an ideal hexagonal A_2BX_n structure ($n = 3$ or 4). It consists of two types of c-axis chains, one composed solely of A atoms, the other of alternating A atoms and BX_n groups. Below T = 745 K the structure becomes slightly orthorhombic but remains unmodulated. We designate this phase P. At $T_o = 130$ K there is a second order transformation to an incommensurate phase I, accompanied by satellite reflections at $\vec{q}_\delta = (1 + \delta)\vec{a}^*/3$ where $\vec{a}^*$ is along the pseudohexagonal axis and $\delta \approx 0.07a^*$. δ decreases with decreasing temperature with a discontinuous jump to $\delta = 0$ at $T_c = 93$ K, tripling the unit cell along $\vec{a}$. We designate this phase F, because a spontaneous ferroelectric polarization also appears in this phase. Iizumi et al. discuss the P → I and I → F transformations using a Landau-type theory in which a term $\sim Q^3(q_\delta)P_z(q_{3\delta})$ plays an essential role in driving the I → F transformation and in inducing the spontaneous polarization. Here $Q(q_\delta)$ is the amplitude of the primary order parameter with wave vector $\vec{q}_\delta$ and $P_z(q_{3\delta})$ is the amplitude of the polarization wave with wave vector $\vec{q}_{3\delta} = 3\delta(\vec{a}^*/3)$. P_z becomes the macroscopic ($\vec{q} = 0$) polarization below T_c.

Whereas all of the CDW transformations in metals studied thus far do not follow the prediction of a simple soft mode instability, $\omega \to 0$ at $T = T_o$, such a simple soft mode behavior is seen above T_o in K_2SeO_4. Fig. 14 shows the dispersion of one of the TA phonon branches (Σ_3) and of the lowest optic phonon branch (Σ_2) for modes propagating along $\vec{a}^*$ in an extended zone scheme at several temperatures. The solid lines are the results of fitting the dispersion relation by the Fourier series

$$\omega^2(\vec{q}) = \sum_n (1 - \cos n\vec{q}) \quad .$$

The coefficients F_n correspond to effective force constants coupling together entire layers of atoms in the crystal separated by 1/2 na. The fits shown in Fig. 14 are unusual in that forces with $n > 3$ are insignificant, but F_1 and F_2 are rather weak and decrease with decreasing temperature in comparison to a strong F_3 which increases with decreasing temperatue, as shown in Fig. 15. There is at present no microscopic understanding of this behavior. The scattering intensity due to the soft $\vec{q}_\delta$-phonon mode was measured about different reciprocal lattice positions and this reveals the soft mode to be primarily a translation of the K^+ ions coupled with rotational motion of the SeO_4 groups.

4.2. Others

There are a rather large number of examples of incommensurate structures which have been reported in the crystallographic literature. Electron diffraction is an ideal way of discovering weak incommensurate satellite reflections. Among the materials for which follow up studies using neutrons have been made are the following.

4.2.1. Thiourea

Between the ferroelectric phase, I, ($T < -104°C$) and the normal paraelectric phase, V, ($T > -71°C$), dielectric measurements indicate three additional phases (II,III,IV). I and V have orthorhombic unit cells of the same size. All of the intermediate phases have satellites of the form $(h,k,\ell+n\delta)$ with $n=0,1,2....$[41] δ seems to vary smoothly with temperature from about 1/8 near -71°C to about 1/10 near -104°C. The displacements appear to be perpendicular to the modulation wave vector. Presumably the ferroelectric transition, which is strongly first order, results from lock in to $\vec{q}=0$, but there is no understanding at present of the nature of the II-III and III-IV transformations, although it must be remarked that III is itself weakly ferroelectric with $P_s \sim 10^{-3}$ that of phase I. Critical scattering in the paraelectric phase is quasielastic and has been interpreted as due to an overdamped transverse phonon, but a softening phonon branch has not apparently been directly observed.[42]

4.2.2. $BaMnF_4$

On the basis of optical and acoustic studies[43,44], it was assumed that the structural transformation at $T_o = 247$ K involved the condensation of a $\vec{q} = (0,1/2,1/2)$ phonon due to rotation of MnF_4 octahedra about the b-axis. However, the neutron scattering investigation of Shapiro et al.[45] shows the principal modulation wave vector to be (0.392,1/2,1/2). There is as yet no determination of the nature of the static distortions nor of the dynamics of the transformation.

4.2.3. $(NH_4)_2BeF_4$

This material is closely related to K_2SeO_4 from a structural point of view. It undergoes two phase transformations at $T_o = 181$ K and $T_c = 175$ K respectively. A spontaneous ferroelectric moment appears below T_c and it was thought that the transformation at T_o involved a commensurate superlattice with $\vec{q} = 1/2\vec{a}^*$. However, careful elastic neutron scattering measurements by Iizumi and Gesi[46] has established that $\vec{q} = (1/2-\delta)\vec{a}^*$ between T_o and T_c with $\delta(T) \rightarrow 0$ discontinuously at T_c. As with K_2SeO_4, the ferroelectricity below T_c can be explained by anharmonic coupling terms in a Landau free energy.

4.2.4. $Hg_{3-\delta}AsF_6$

This remarkable material can be thought to consist of an ordered tetragonal AsF_6 lattice in which there are open non-intersecting channels running parallel to both basal plane edges. These channels are filled with tightly packed chains of Hg ions. The observed interchain Hg-Hg distance is such that $3-\delta(\delta \approx 0.18)$ Hg ions can be accommodated within a unit cell of the AsF_6 lattice.[47,48] At high temperatures the phase relation between the Hg chains is random, but below $T_o = 120$ K Hastings et al.[49], find a phase transformation into an incommensurate structure where the phase relation between adjacent Hg chains is staggered so as to produce a net interaction between sets of chains running in orthogonal directions. A "one-dimensional" phonon dispersion curve associated with the random Hg chains has been measured at room temperature.

5. CONCLUDING REMARKS

Our understanding of incommensurate structures is in a developing and therefore interesting phase. From a static or structural point of view experiment has often preceded theory, particularly in the discovery of the rather rich and subtle area of lock-in transformations. Although these phenomena were not anticipated by theory, they seem to raise no fundamental puzzles in their understanding. By contrast, an adequate theoretical understanding is lacking for the failure of the phonon mode to soften completely for CDW instabilities in metals, although the existing data suggest that this may be generally true. We have focused attention on the phonon behavior above T_0, but the situation below T_0 promises to be more interesting. Because it is possible to make a shift in the overall phase of the CDW condensate in an incommensurate structure with no change in energy, there should appear a new kind of gapless excitation branch (phason) which may contribute to interesting and unusual transport and thermal properties.[50,51] Undoubtedly, neutron scattering will continue to play a major role in further work in this area.

6. ACKNOWLEDGMENTS

The author appreciates the help and advice of many of his colleagues, especially R. Comès, F. Di Salvo, M. Iizumi, D. E. Moncton, and G. Shirane, in preparing this review.

REFERENCES

[1] COCHRAN, W., Adv. Phys. 9 (1960) 387.
[2] COCHRAN, W., ZIA, A. phys. stat. sol. 25 (1968) 273.
[3] OVERHAUSER, A. W., Phys. Rev. 167 (1968) 691.
[4] KOHN, W., Phys. Rev. Lett. 2 (1959) 393.
[5] DENLEY, D. and FALICOV, L. M., to be published.
[6] deWOLFF, P. M., Acta Cryst. A30 (1974) 777.
[7] JANNER, A. and JANSSEN, T., Phys. Rev. B 15 (1977) 643.
[8] WILSON, J. A., DI SALVO, F. J., and MAHAJAN, S., Adv. in Phys. 24 (1975) 117.
[9] DI SALVO, F. J., "Electron Phonon Interactions and Phase Transitions" NATO Advanced Study Institute Series, Ed. T. RISTE, to be published.
[10] MONCTON, D. E., AXE, J. D., DI SALVO, F. J., Phys. Rev. B 16 (1977) 801; Phys. Rev. Lett. 34 (1975) 734.
[11] DI SALVO, F. J., MONCTON, D. E. WILSON, J. A., and MAHAJAN, S. Phys. Rev. B 14 (1976) 1543.
[12] MONCTON, D. E., DI SALVO, F. J., AXE, J. D., PATTON, B. R. and SHAM, L. J., Phys. Rev. B 14 (1976) 3432.
[13] PEIERLS, R. F., "Quantum Theory of Solids," Clarendon Press, Oxford (1955).
[14] Lecture Notes in Physics, Vol. 34, "One-Dimensional Conductors" (Springer, New York, 1975).
[15] "Chemistry and Physics of One-Dimensional Metals," Ed. H. J. KELLER (Plenum Press, New York, 1977).
[16] COMES, R. and SHIRANE, G., "Highly Conducting One-Dimensional Solids," Ed. J. T. DEVREESE (Plenum) to be published.
[17] COMES, R., LAMBERT, M., LAUNOIS, H., and ZELLER, H. R., Phys. Rev. B 8 (1973) 571.
[18] RENKER, B., PINTSCHOVIUS, L., GLASER, W., RIETSCHEL, H., COMES, R., LIEBERT, L., and DREXEL, W., Phys. Rev. Lett. 32 (1974) 836.
[19] COMES, R., RENKER, B., PINTSCHOVIUS, L., CURRAT, R., GLASER, W., and SCHREIBER, G., phys. stat. sol. (b) 71 (1975) 171.
[20] CARNEIRO, K., SHIRANE, G., WERNER, S. A., and KAISER, S., Phys. Rev. B 13 (1976) 4258.
[21] LYNN, J. W., IIZUMI, M., SHIRANE, G., WERNER, S. A., and SAILLANT, R. B., Phys. Rev. B 12 (1975) 1154.
[22] IMRY, Y., PINCUS, P., SCALAPINO, D. J., Phys. Rev. B 12 (1975) 1978.
[23] COLEMAN, L. B., COHEN, M. J., SANDMAN, D. J., YAMAGISHI, F. G., GARITO, A. F., and HEEGER, A. J., Solid State Commun. 12 (1973) 1125.
[24] DENOYER, F., COMES, R., GARITO, A. F., and HEEGER, A. J., Phys. Rev. Lett. 35 (1975) 445.
[25] KAGOSHIMA, S., ANZAI, H., KAJIMURA, K., and ISHIGORO, T., J. Phys. Soc. Japan 39 (1975) 1143.
[26] COMES, R., SHAPIRO, S. M., SHIRANE, G., GARITO, A. F., and HEEGER, A. J., Phys. Rev. Lett. 35 (1975) 1518; Phys. Rev. B 14 (1976) 2376.
[27] ELLENSON, W. D., COMES, R., SHAPIRO, S. M., SHIRANE, G., GARITO, A. F. and HEEGER, A. J., Solid State Commun. 20(1976) 53.
[28] ELLENSON, W. D., SHAPIRO, S. M., SHIRANE, G. and GARITO, A. F., Phys. Rev. (to be published).
[29] KISTENMACHER, T. J., PHILLIPS, T. E. and COWAN, D. O., Acta Cryst. B 30 (1974) 763.
[30] BAK, P., and EMERY, V. J., Phys. Rev. Lett. 36 (1976) 978.
[31] SCHULTZ, T. D. and ETEMAD, S., Phys. Rev. B 13 (1976) 4928.

[32] ABRAHAMS, E., SOLYOM, J. and WAYNAROVICH, F., to be published.
[33] SHIRANE, G., SHAPIRO, S. M., COMES, R., GARITO, A. F., and HEEGER, A. J., Phys. Rev. B 14 (1976) 2325.
[34] SHAPIRO, S. M., SHIRANE, G., GARITO, A. F., and HEEGER, A. J., Phys. Rev. B 15 (1977) 2413.
[35] POUGET, J. P., KHANNA, S. K., DENOYER, F., COMES, R., GARITO, A. F. and HEEGER, A. J., Phys. Rev. Lett. 37 (1976) 437.
[36] KAGOSHIMA, S., ISHIGURO, T., and ANZAI, H. J. Phys. Soc. Japan 41 (1976) 2061.
[37] MOOK, H. A. and WATSON, C. R., Phys. Rev. Lett. 36 (1976) 801.
[38] MOOK , H. A., SHIRANE, G. and SHAPIRO, S. M., to be published.
[39] TORRANCE, J. B., "Chemistry and Physics of One-Dimensional Metals," Ed. H. J. KELLER (Plenum, 1977).
[40] IIZUMI, M., AXE, J. D., SHIRANE, G. , and SHIMAOKA, K., Phys. Rev. B 15 (1977) 4392.
[41] SHIOZAKI, Y., Ferroelectrics 2 (1971) 245.
[42] MCKENZIE, D. R., J. Phys. C8 (1975) 1607.
[43] RYAN, J. F. and SCOTT, J. F., Solid State Commun. 14 (1974) 5.
[44] FRITZ, I. J., Phys. Rev. Lett. 35 (1975) 1511.
[45] SHAPIRO, S.M., COWLEY, R. A., COX, D. E., EIBSCHUTZ, M., and GUGGENHEIM, H. J., "Proceedings of Conference on Neutron Scattering," ERDA CONF-760601-P1, R. M. Moon, Ed., pp. 399-405.
[46] IIZUMI, M. and GESI, K., to be published.
[47] BROWN, I. D., CUTFORTH, B. D., DAVIES, C. G., GILLESPIE, R. J. IRELAND, P. R., and VEKRIS, J. E., Can. J. Chem. 52 (1974) 791
[48] SCHULTZ, A. J., WILLIAMS, J. M., MIRO, N. D., MACDIARMID, A. G., and HEEGER, A. J., Inorganic Chemistry (submitted).
[49] HASTINGS, J. M., POUGET, J. P., SHIRANE, G., HEEGER, A. J., MIRO, N. D., and MACDIARMID, A. G., Phys. Rev. Lett. (submitted).
[50] OVERHAUSER, A. W., Phys. Rev. B 3 (1971) 3173.
[51] FRÖHLICH, H. Proc. Roy. Soc. A 223 (1954) 296.

FIGURE CAPTIONS

Fig. 1. Temperature dependence of satellite intensities in $TaSe_2$ and $NbSe_2$. (after Ref. 10).

Fig. 2. Temperature dependence of the satellite wave vector, $\vec{q}_\delta = (1-\delta)a^*/3$, in $TaSe_2$ and $NbSe_2$. (after Ref. 10).

Fig. 3. Schematic view of the ionic displacement pattern for $TaSe_2$ at 5 K. Only one of the two layers is shown. Filled circles = Ta, open circles = Se. (after Ref. 10).

Fig. 4. Phonon dispersion relations for Σ_1 phonon branches in $TaSe_2$ and $NbSe_2$. (after Ref. 10).

Fig. 5. Temperature dependence of soft phonon energy in $TaSe_2$. T_o marks the onset of CDW formation. (after Ref. 10).

Fig. 6. The CDW pattern and metal atom positions expected for commensurate 3x1 structure in 1T-TaS_2/Se_2. (after Ref. 8).

Fig. 7. Diffraction patterns illustrating influence of impurities on the stacking sequence of 1T $Ta_{1-x}Zr_xSe_2$. (after Ref. 12).

Fig. 8. Dispersion surface of acoustic phonon in KCP with [001] polarization at room temperature. (after Ref. 19).

Fig. 9. Intensity contours of inelastic scattering in KCP showing extremely sharp Kohn anomaly near $\vec{q} = 0.3\ \vec{c}^*$. (after Ref. 20).

Fig. 10. Peak intensity (solid circles) and width $\perp$ to c-axis (open circles) of the CDW satellites in KCP. (after Ref. 21).

Fig. 11. Schematic structure of TTF-TCNQ, in projection on the AC plane, perpendicular to the 1-d stacks. Bolder lines are at 1/2 $\vec{b}$ above ac plane.

Fig. 12. Temperatue dependence of a*-axis component of satellite positions in TTF-TCNQ. (after Ref. 28).

Fig. 13. Dispersion of acoustic phonons propagating along b* in TTF-TCNQ. (after Ref. 34).

Fig. 14. Dispersion of Σ_2, Σ_3 soft mode branches of K_2SeO_4 in an extended zone scheme. (after Ref. 40).

Fig. 15. Temperature dependence of interlayer force constants in K_2SeO_4. (after Ref. 40).

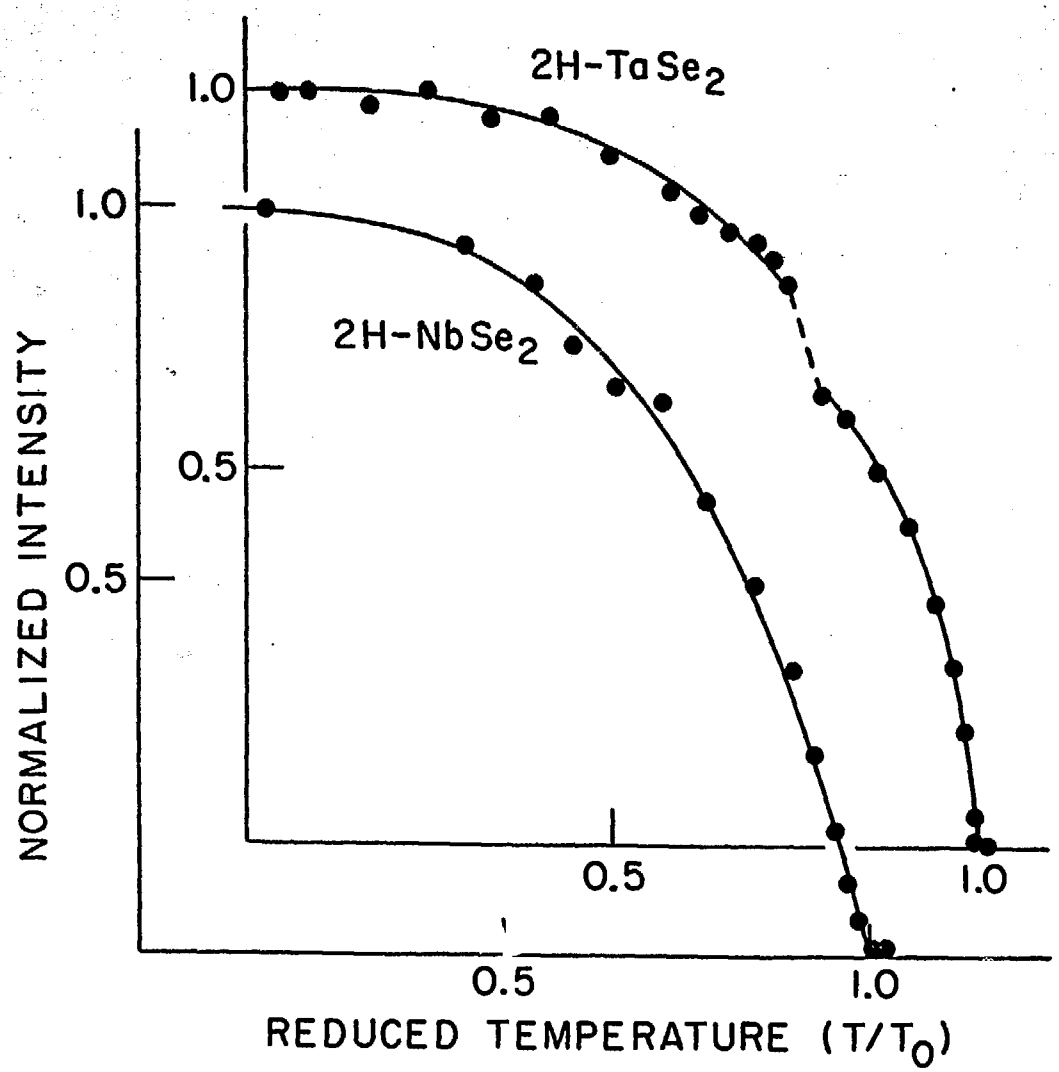

Fig. 1. Temperature dependence of satellite intensities in $TaSe_2$ and $NbSe_2$. (after Ref. 10).

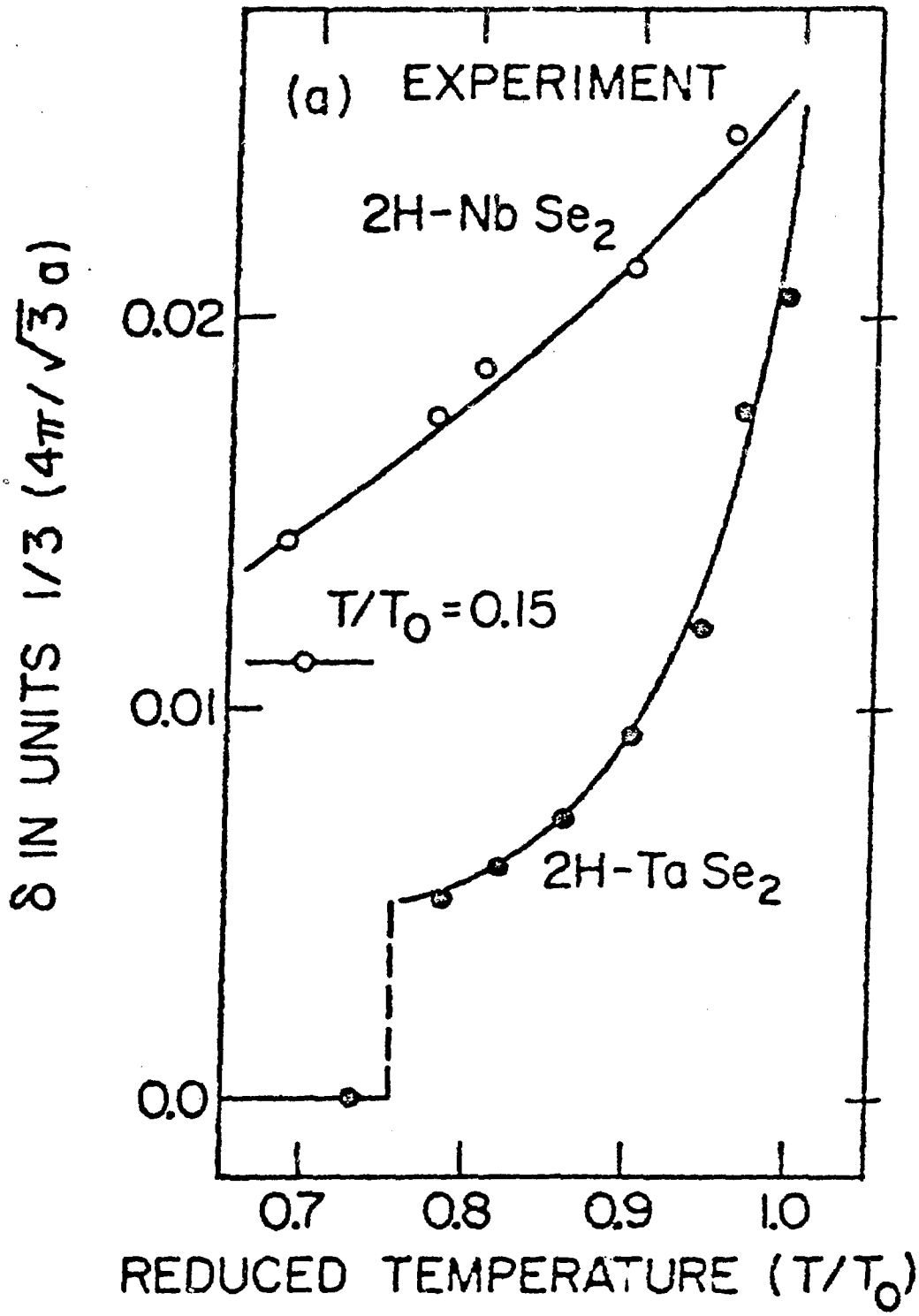

Fig. 2. Temperature dependence of the satellite wave vector, $\vec{q}_\delta = (1-\delta)\vec{a}^*/3$, in $TaSe_2$ and $NbSe_2$. (after Ref. 10).

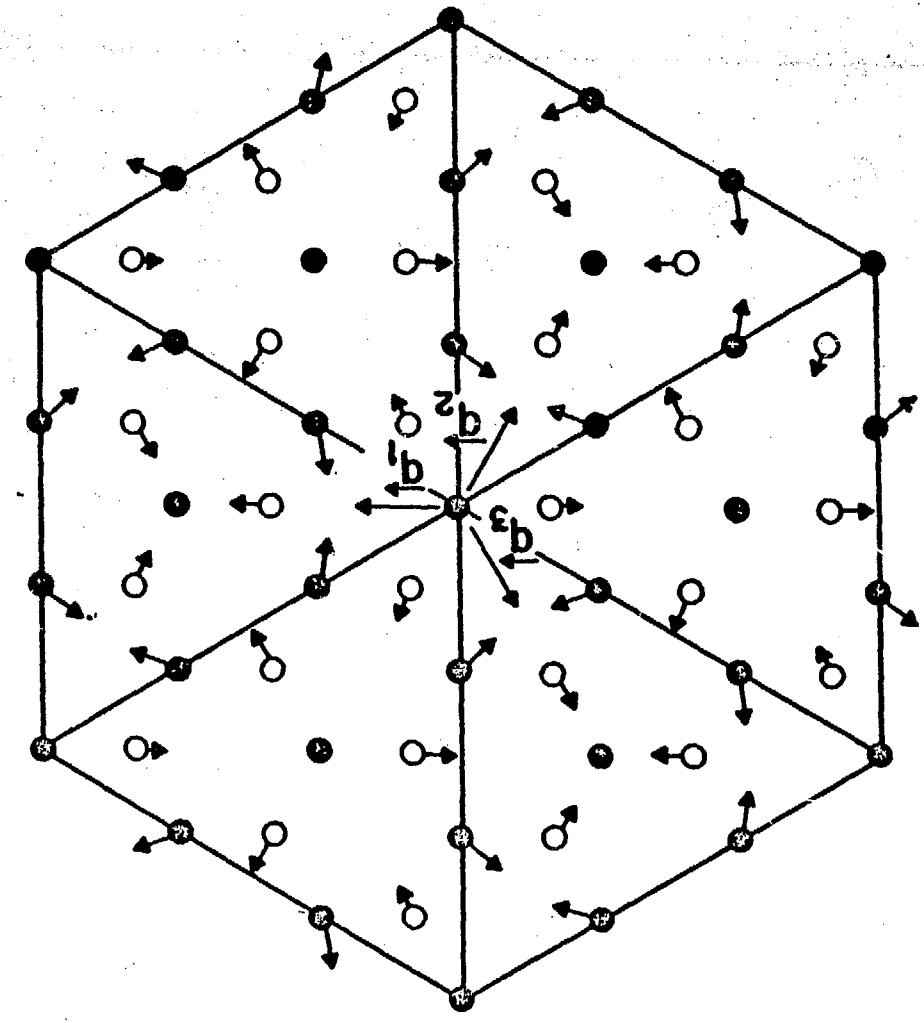

Fig. 3. Schematic view of the ionic displacement pattern for $TaSe_2$ at 5 K. Only one of the two layers is shown. Filled circles = Ta, open circles = Se. (after Ref. 10).

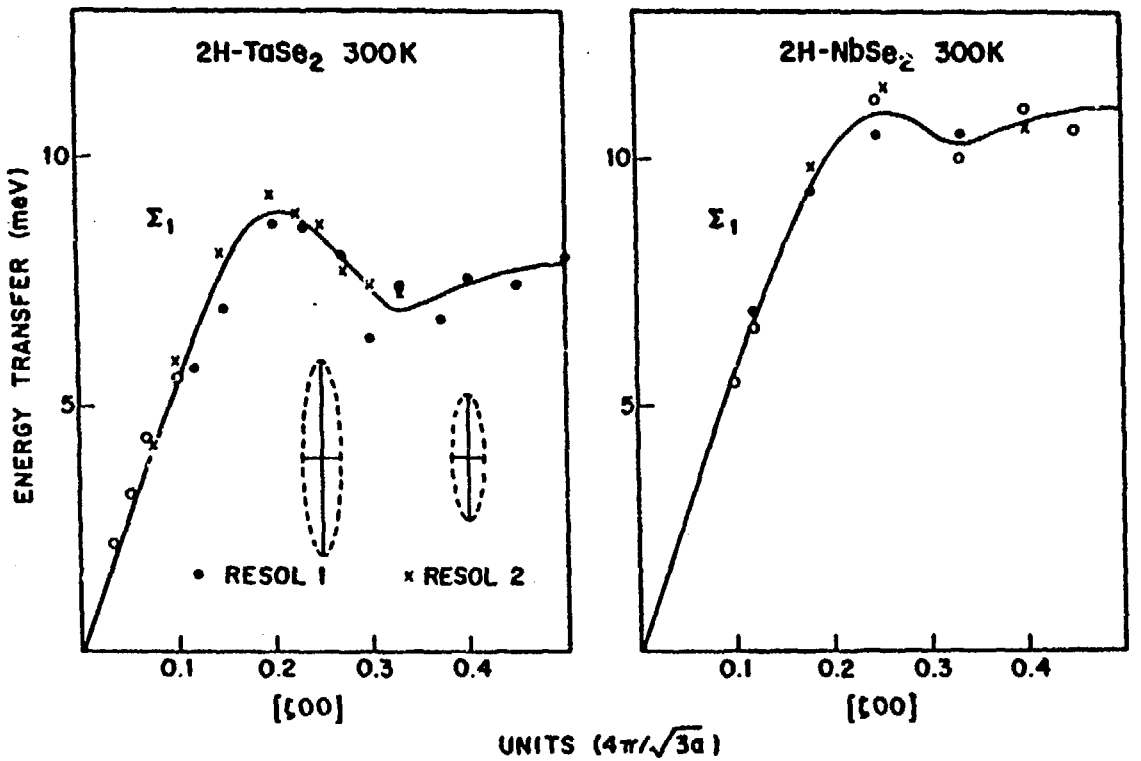

Fig. 4. Phonon dispersion relations for Σ_1 phonon branches in $TaSe_2$ and $NbSe_2$. (after Ref. 10).

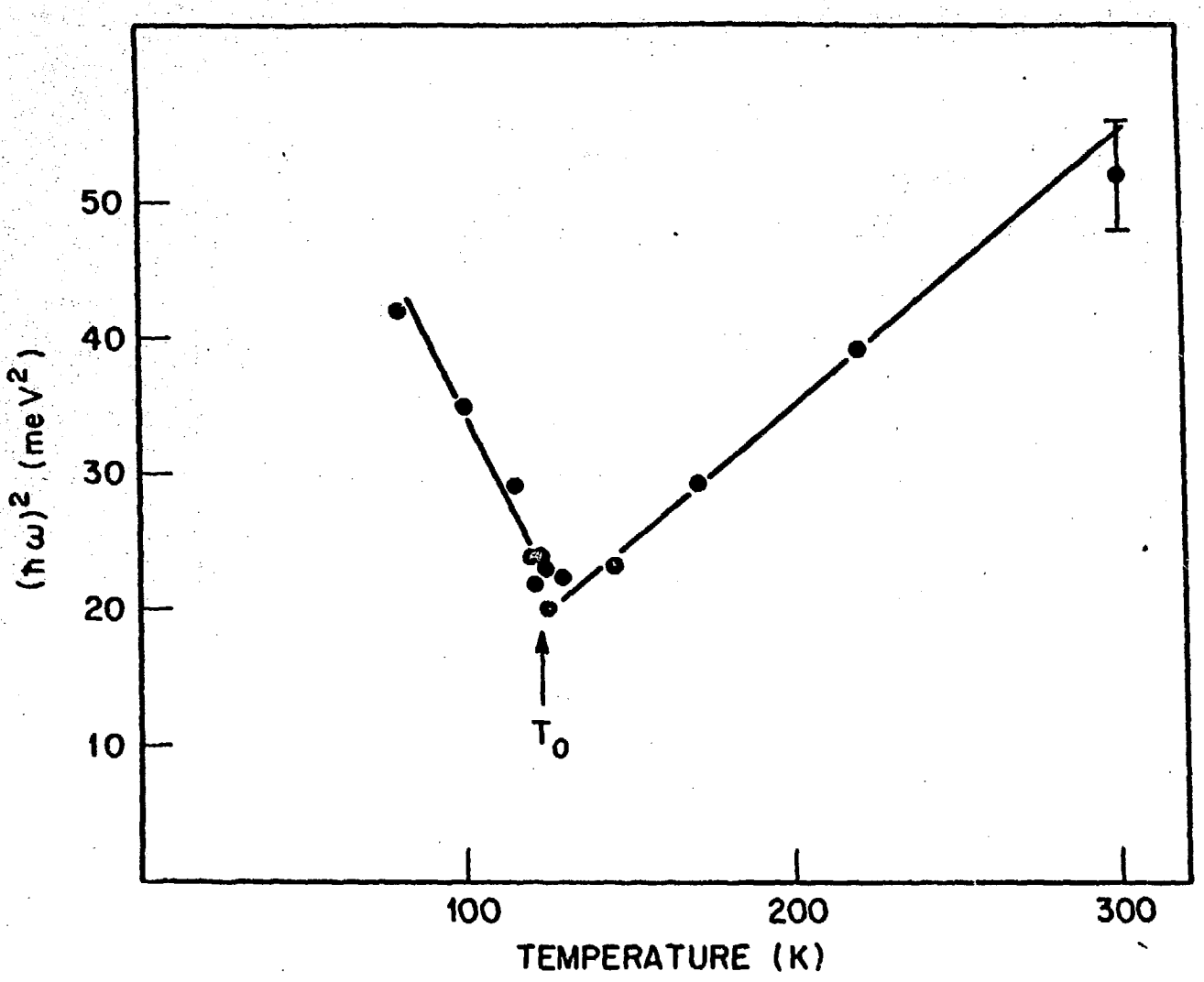

Fig. 5. Temperature dependence of soft phonon energy in $TaSe_2$. T_0 marks the onset of CDW formation (after Ref.10).

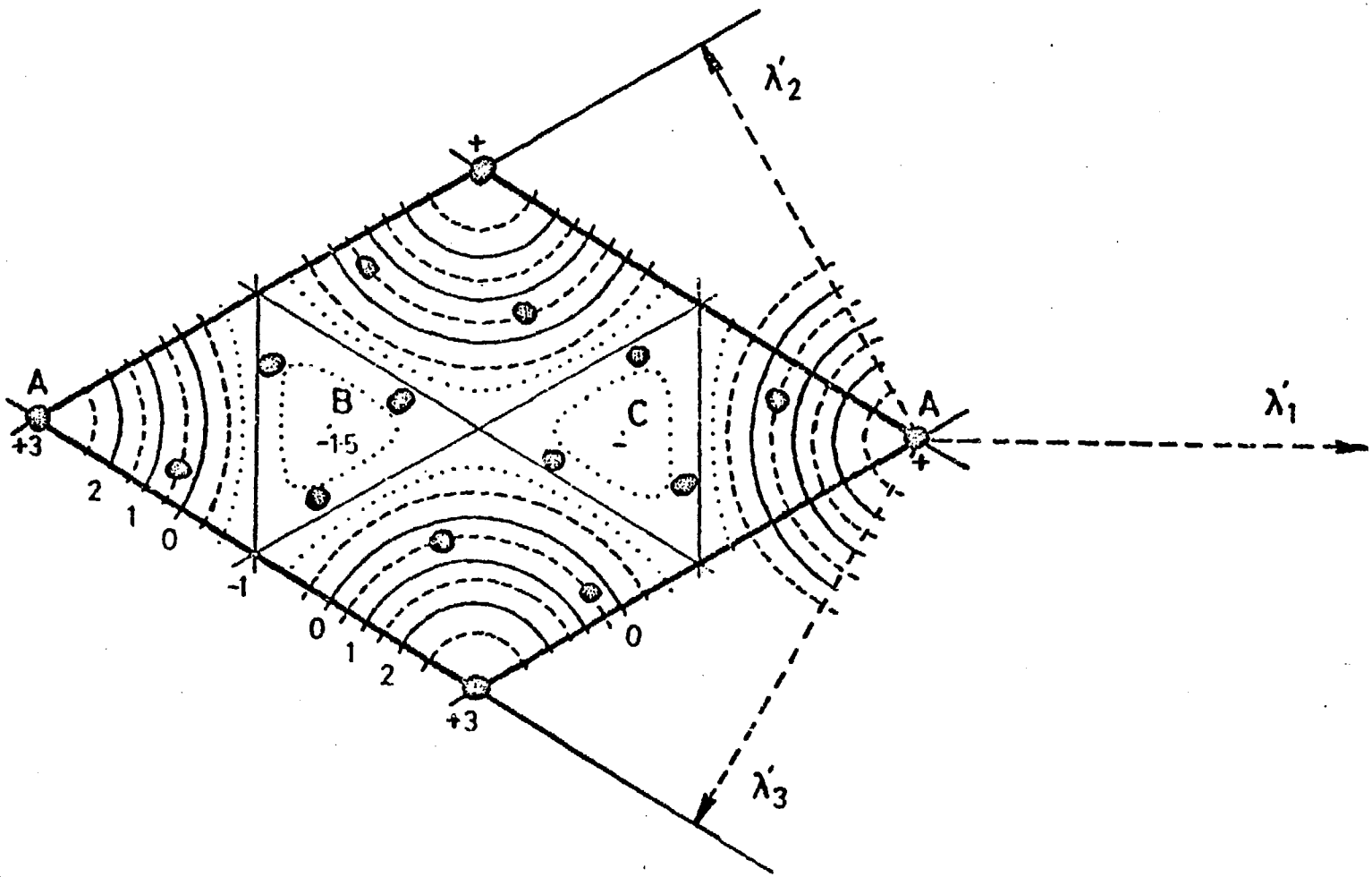

Fig. 6. The CDW pattern and metal atom positions expected for commensurate 3x1 structure in 1T-TaS_2/Se_2. (after Ref. 8).

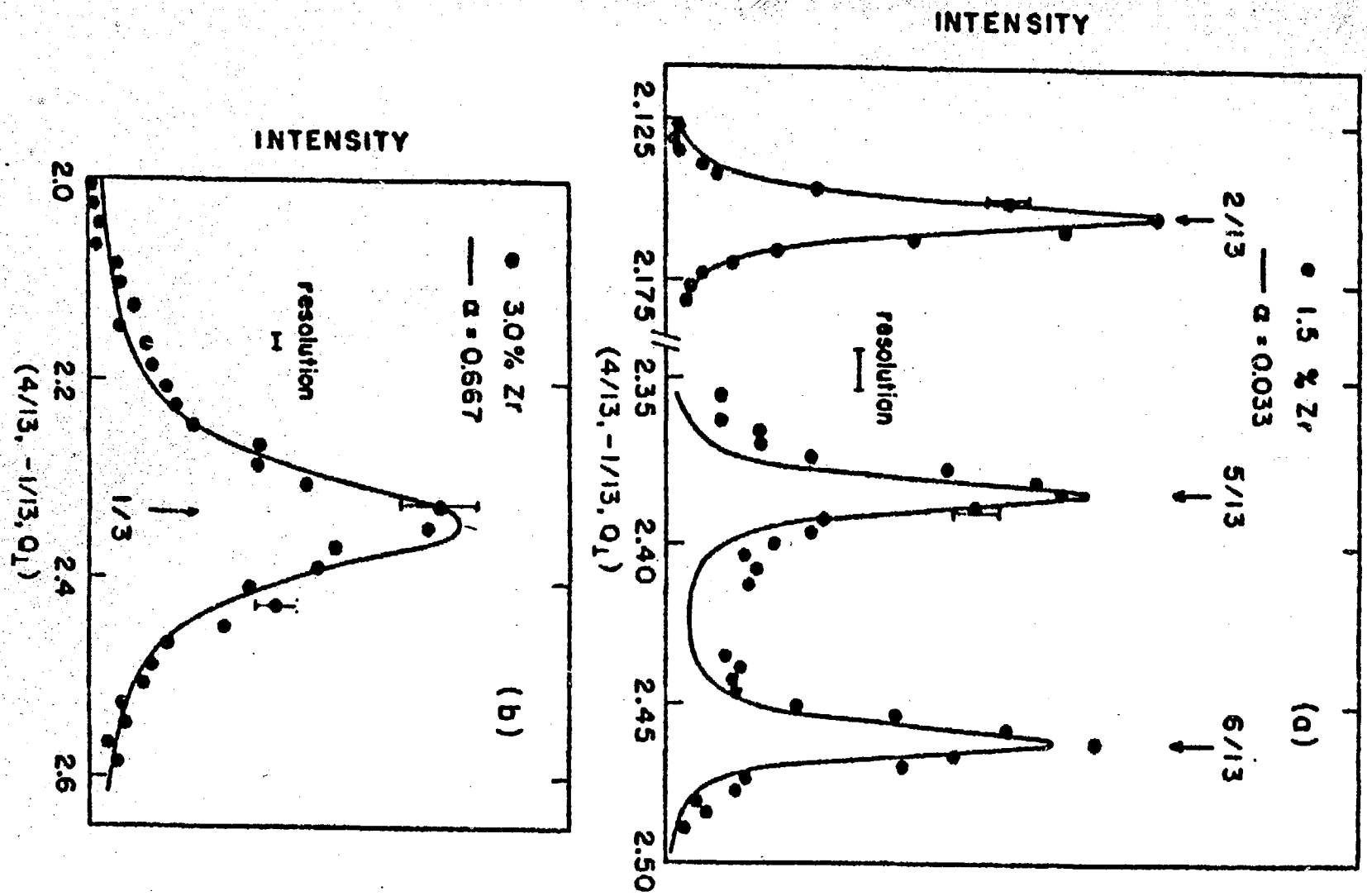

Fig. 7. Diffraction patterns illustrating influence of impurities on the stacking sequence of 1T-$Ta_{1-x}Zr_xSe_2$. (after Ref. 12).

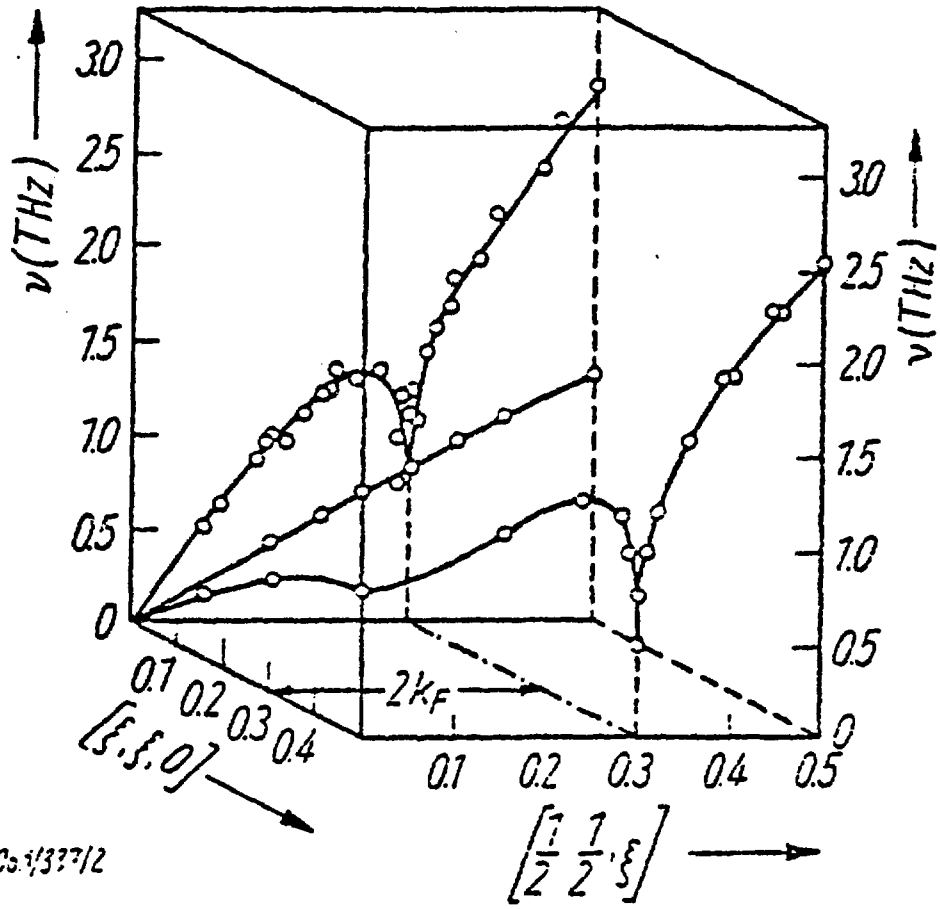

Fig. 8. Dispersion surface of acoustic phonon in KCP with [001] polarization at room temperature. (after Ref. 19).

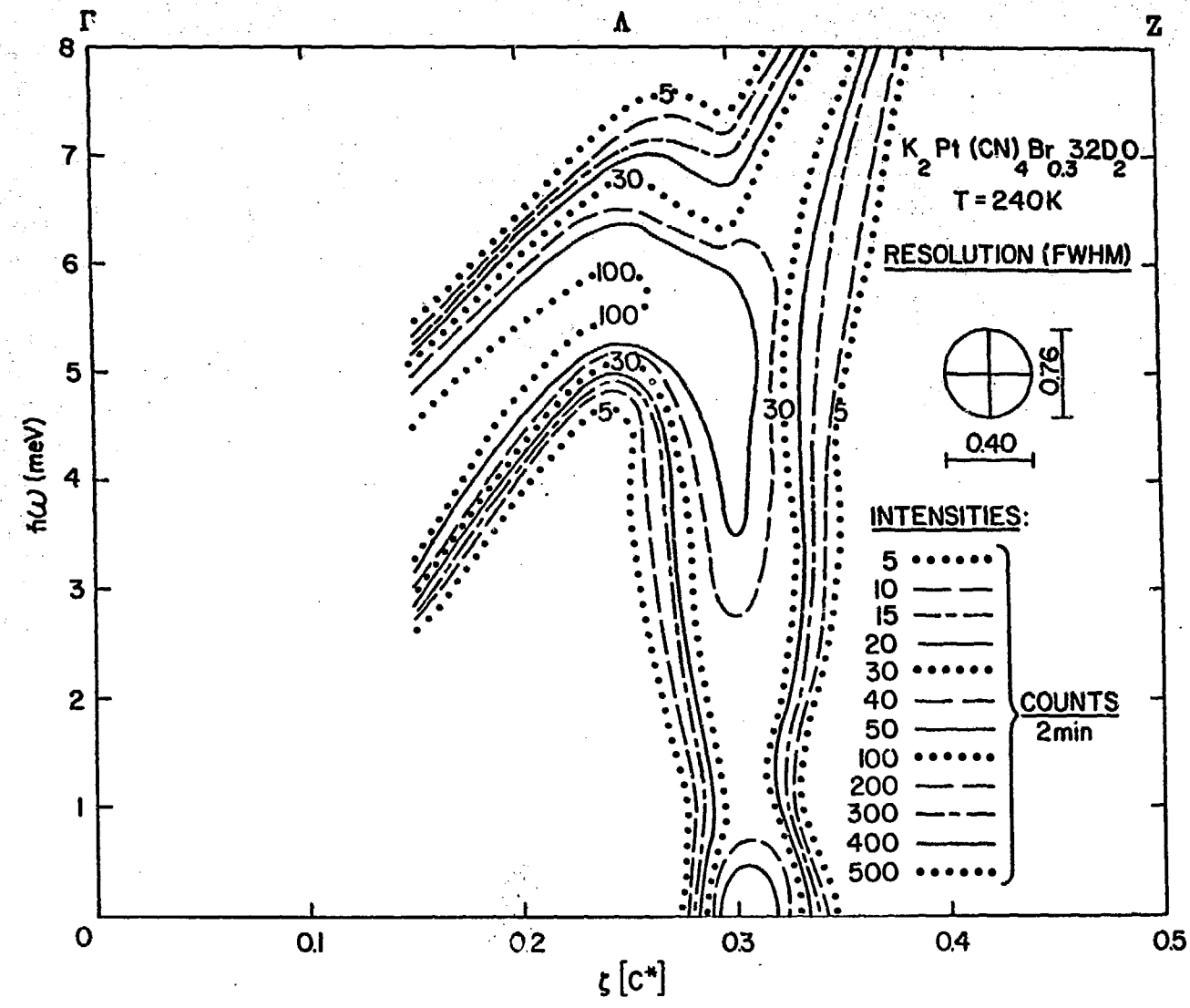

Fig. 9. Intensity contours of inelastic scattering in KCP showing extremely sharp Kohn anomaly near $\vec{q} = 0.3\vec{c}^*$. (after Ref. 20).

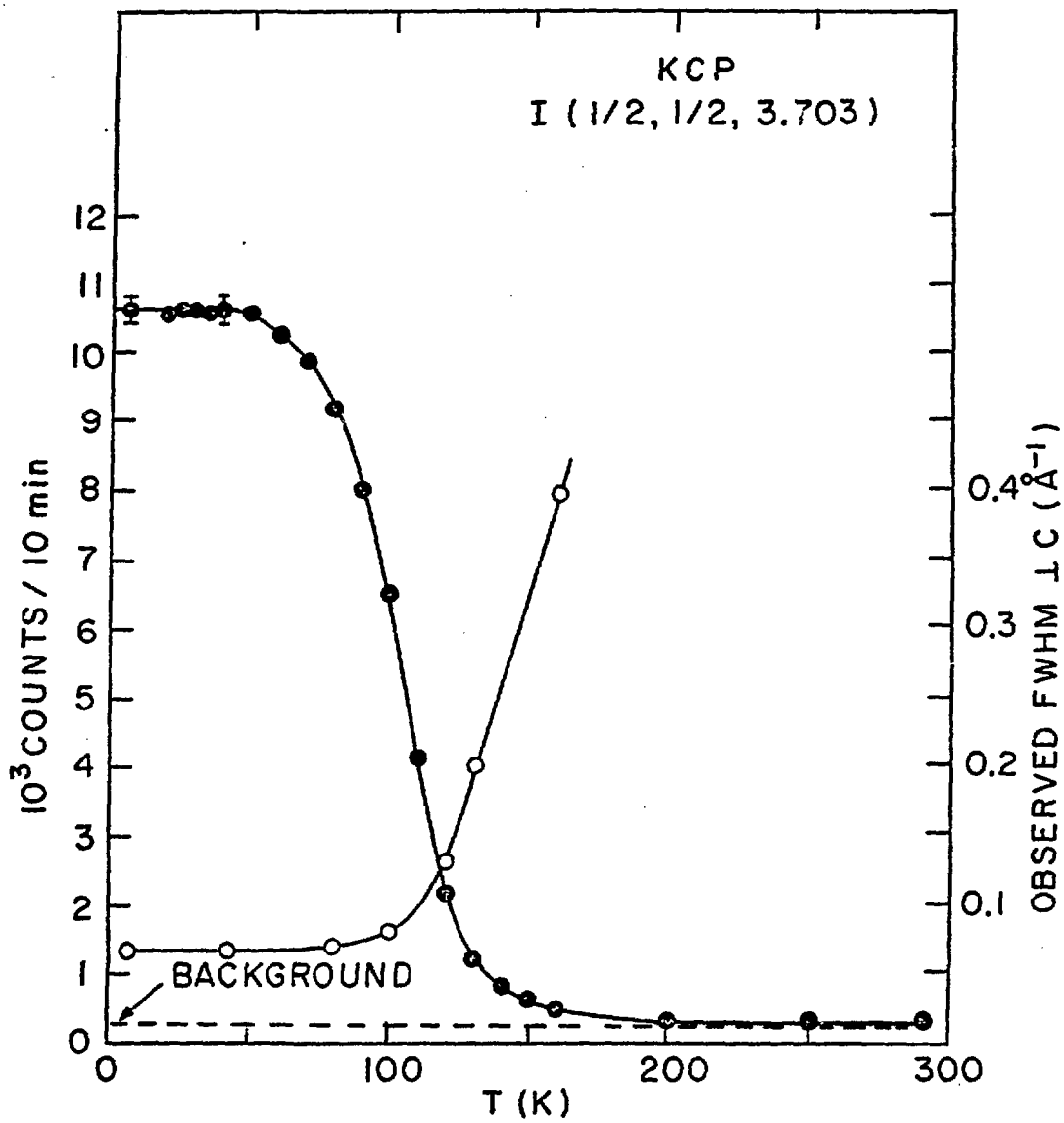

Fig. 10. Peak intensity (solid circles) and width ⊥ to c-axis (open circles) of the CDW satellites in KCP. (after Ref. 21).

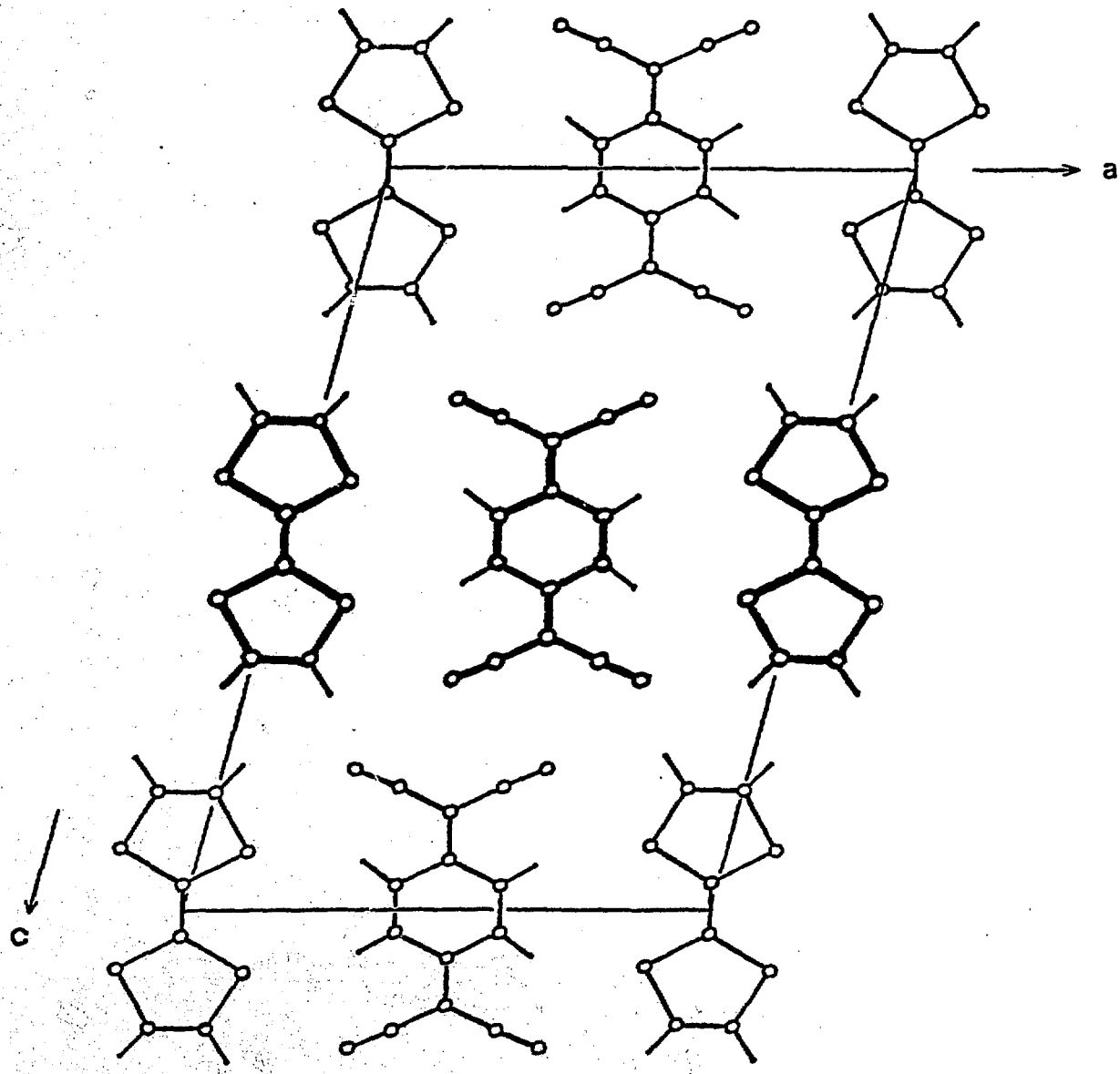

Fig. 11. Schematic structure of TTF-TCNQ, in project on the AC plane, perpendicular to the 1-d stacks. Bolder lines are at 1/2 $\vec{b}$ above ac plane.

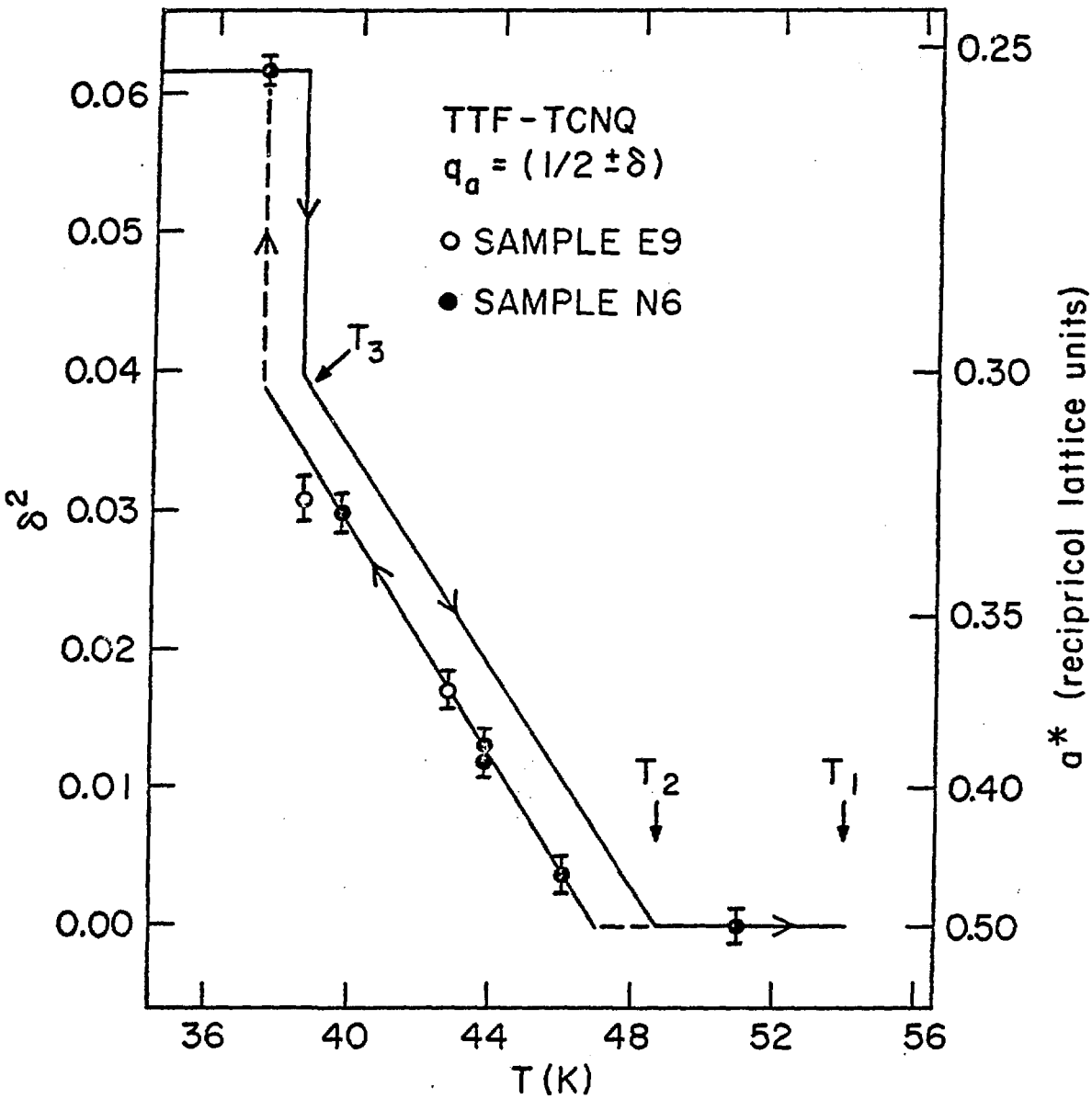

Fig. 12. Temperature dependence of a*-axis component of satellite positions in TTF-TCNQ. (after Ref. 28).

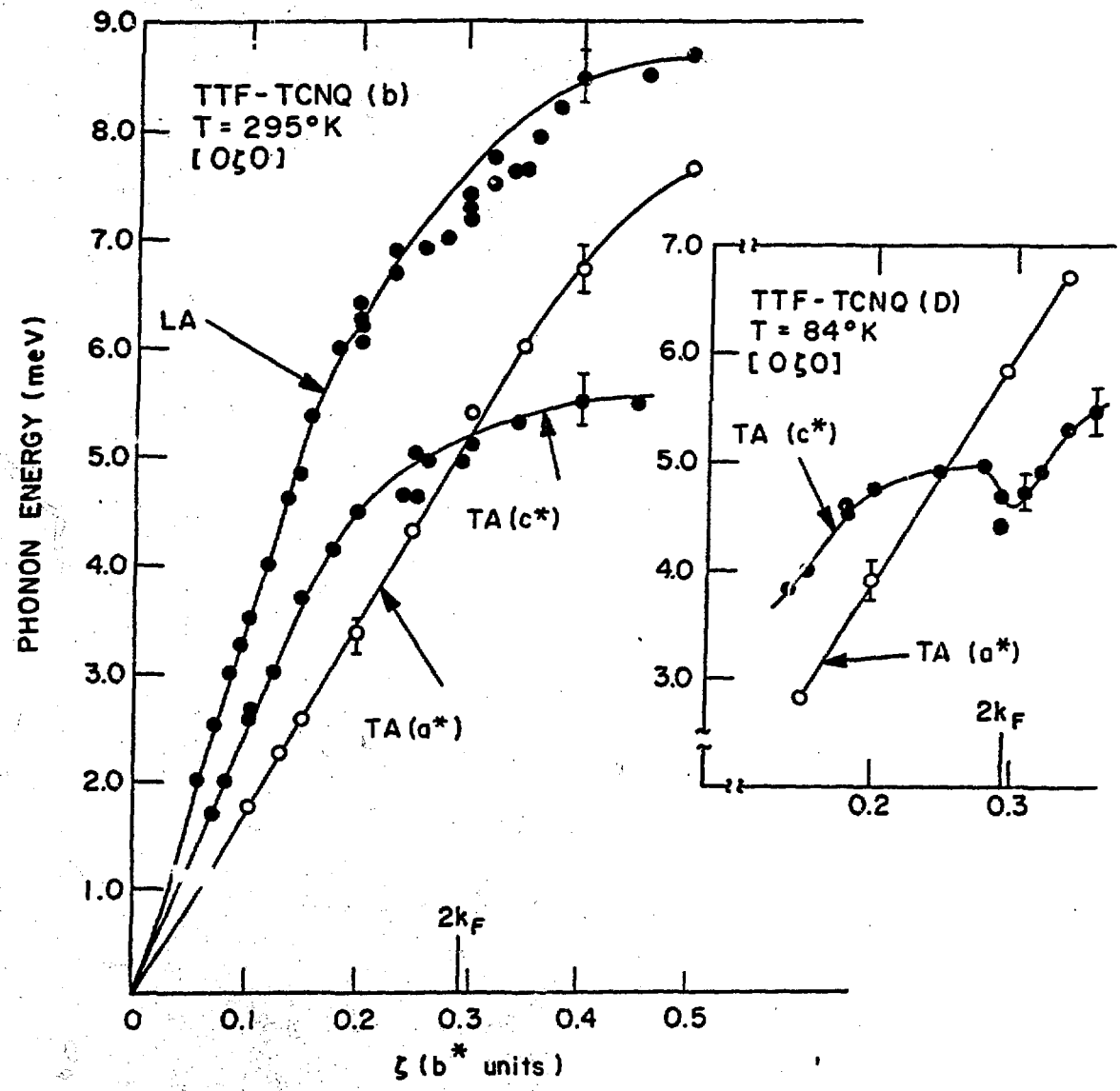

Fig. 13. Dispersion of acoustic phonons propagating along b* in TTF-TCNQ. (after Ref. 34).

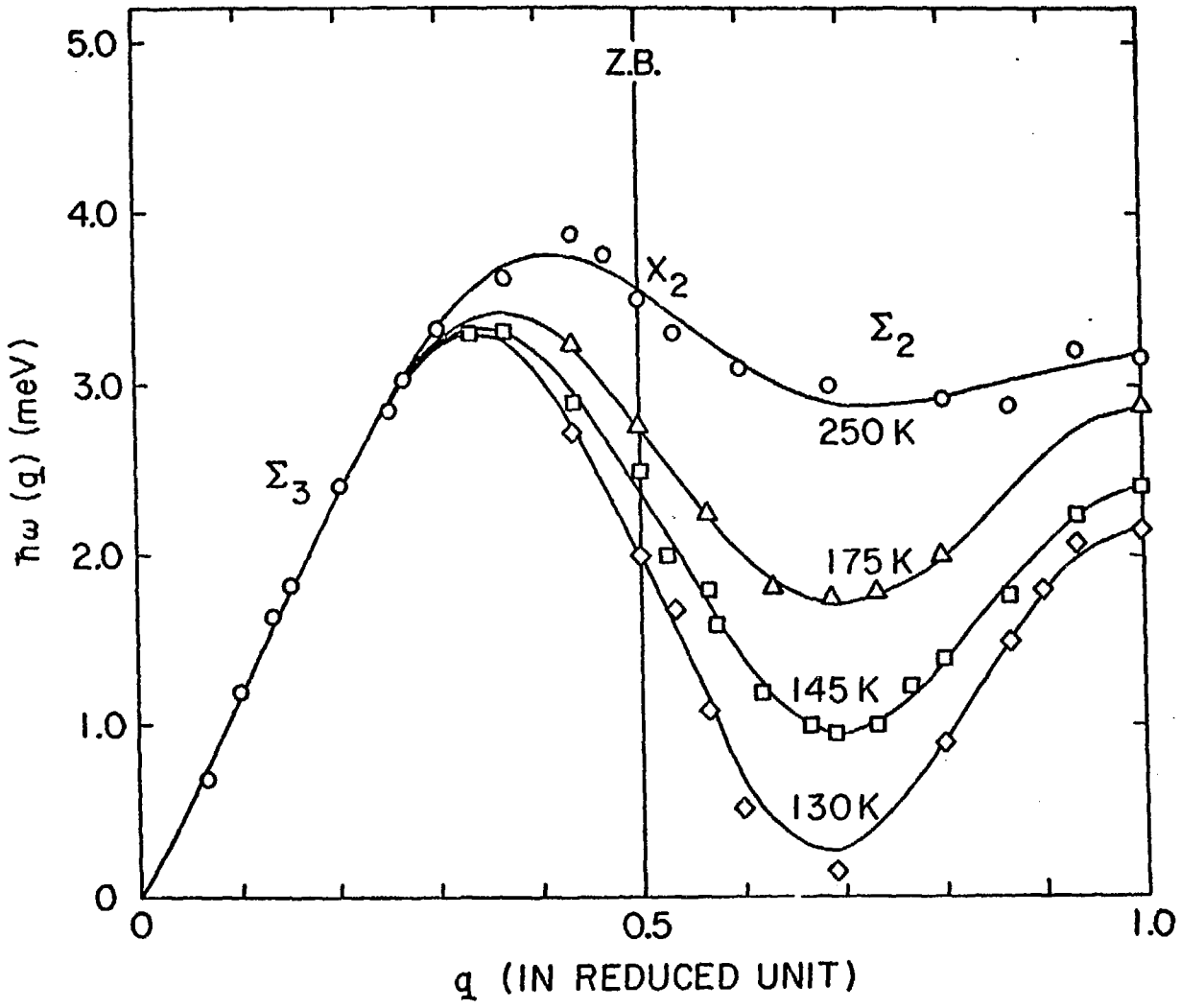

Fig. 14. Dispersion of Σ_2, Σ_3 soft mode branches of K_2SeO_4 in an extended zone scheme. (after Ref. 40).

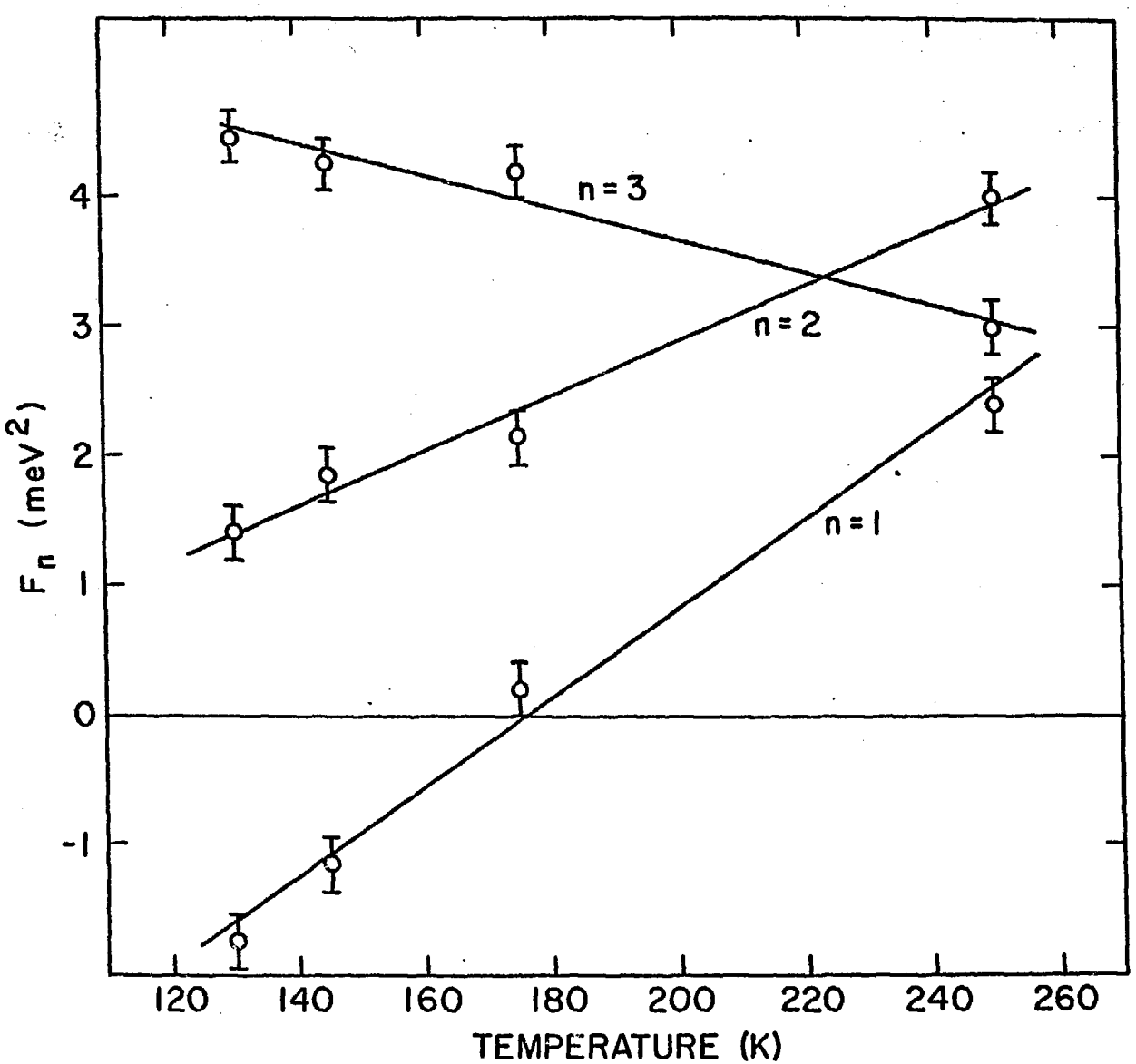

Fig. 15. Temperature dependence of interlayer force constants in K_2SeO_4. (after Ref. 40).